Comparative Medicine
Copyright 2009
by the American Association for Laboratory Animal Science

Vol 59, No 3
June 2009
Pages 266–271

Assessing Anticalcification Treatments in Bioprosthetic Tissue by Using the New Zealand Rabbit Intramuscular Model

Gregory A Wright,* Joelle M Faught, and Jane M Olin

The objective of this work was to demonstrate that the New Zealand White (NZW) rabbit intramuscular model can be used for detecting calcification in bioprosthetic tissue and to compare the calcification in the rabbit to that of native human valves. The rabbit model was compared with the commonly used Sprague–Dawley rat subcutaneous model. Eighteen rabbits and 18 rats were used to assess calcification in bioprosthetic tissue over time (7, 14, 30, and 90 d). The explanted rabbit and rat tissue discs were measured for calcium by using atomic absorption and Raman spectroscopy. Calcium deposits on the human valve explants were assessed by using Raman spectroscopy. The results showed that the NZW rabbit model is robust for detecting calcification in a shorter duration (14 d), with less infection complications, more space to implant tissue groups (thereby reducing animal use numbers), and a more metabolically and mechanically dynamic environment than the rat subcutaneous model . The human explanted valves and rabbit explanted tissue both showed Raman peaks at 960 cm^{-1} which is representative of hydroxyapatite. Hydroxyapatite is the final calcium and phosphate species in the calcification of bioprosthetic heart valves and rabbit intramuscular implants. The NZW rabbit intramuscular model is an effective model for assessing calcification in bioprosthetic tissue.

Abbreviations: BHV, bioprosthetic heart valve; FET, formaldehyde–ethanol–Tween 80; NZW, New Zealand White.

Because of their outstanding durability, mechanical heart valves were 1 of the first replacement valves used in humans. However, drawbacks to mechanical valves include patient complaints regarding the noise the valve makes and the risk of lifelong anticoagulation therapy.[4,20] Currently bioprosthetic heart valves (BHV) are 1 of the most common medical devices used to replace damaged mitral and aortic heart valves in men and women 65 y and older.[17]

A leading drawback to BHV is dystrophic calcification, which is typically the primary failure mode for these devices.[15] Calcification in BHV is believed to be caused by multiple factors, with glutaraldehyde (used to crosslink the tissue), residual cellular debris, and mechanical stress as the major factors. Patient factors including diabetes, renal failure, atherosclerosis, and calcium metabolism disorders can be important contributors as well.[14] BHV are designed by using bovine pericardium, porcine valve leaflets, and porcine pericardium or dura mater; the most common tissues used are bovine pericardium and porcine valve leaflets.[36] Preventing or delaying calcification of BHV is an ongoing research dilemma of biomedical device companies. A 1982 study assessed explanted human valves that had been treated with glutaraldehyde only and found that calcification was the main cause of valve explantation and valves typically lasted only 9 1/2 y on average.[3] To increase the durability and delay the onset of calcification of glutaraldehyde-treated valves, researchers and heart valve manufacturers began developing anticalcification treatments. In early studies, chemical compounds like protamine were used to block charged chemical groups and thus reduce calcification in glutaraldehyde-treated BHV.[13] Other treatments used ethanol, $AlCl_3$, $FeCl_3$, L-Hydro, and osteopontin.[11,23,25,35] Many of these treatments were either proven ineffective or were not able to be manufactured. Effective new anticalcification treatments currently available commercially include α-amino oleic acid (Medtronic, Minneapolis, MN), an ethanol-based treatment (Linx, St Jude Medical, St Paul, MN), and a process involving formaldehyde, ethanol, and Tween 80 (ThermaFix, Edwards Lifesciences, Irvine, CA).[10,12] However, young adolescents and patients with calcium metabolic disorders still receive mechanical valves due to rapid calcification of BHV implants in these patient groups.[26]

An animal model is necessary to assess the effects of anticalcification treatments on bioprosthetic tissue in a short and effective timeframe. When assessing anticalcification tissue treatments, the animal models used are typically rats and rabbits. Wistar and Sprague–Dawley rats and New Zealand White (NZW) rabbits are the strains of choice.[5,29] Small animals are chosen because they are inexpensive, the tissue calcifies in a short period of time, the surgical procedure requires minimal pain and discomfort, and the animals are easy to care for.[9] Typically, the BHV leaflet tissue is cut into discs or is used as whole leaflets and implanted subcutaneously in either rats or rabbits. Typical study duration to assess anticalcification efficacy in the rat model varies from 90 d to 6 mo.[24,41] The Sprague–Dawley rat is one of the most common models used to assess BHV tissue calcification properties.[27] The NZW rabbit model is another small animal model available, but to date only the subcutaneous route has been used for tissue biocompatibility and toxicology in drug efficacy studies only.

Received: 18 Nov 2008. Revision requested: 23 Dec 2008. Accepted: 02 Mar 2009.
Research and Development, Edwards Lifesciences, Irvine, California.
**Corresponding author. Email: Biogregw71@hotmail.com*

Large animal models used to assess the safety and efficacy of BHV have included pig, sheep, cows, and nonhuman primates, but the primary model currently used is the juvenile sheep.[38] The juvenile sheep is a robust model that performs similarly to humans with regards to hemodynamics, valve annulus sizing, and thrombogenicity.[1,10] A typical safety and efficacy study in juvenile sheep lasts 20 wk.[21] The drawbacks to using sheep to assess anticalcification treatments are the large sample size needed to demonstrate statistically significant differences, high surgical costs, and high animal-care costs.

The age of the animal is important when assessing the calcification potential of BHV tissue. Compared with their older counterparts, juvenile animals demonstrate higher calcium metabolism because of bone-building, organ function, and structural tissues.[7] Ways to assess calcium metabolism in small animals include measuring skeletal length and bone growth relative to sexual maturation.[32] In Wistar rats, bone growth increased from 276 µm/d in 21-d-old weanlings to 330 µm/d in 35-d-old rats.[19,42] The bone growth spurt in the rats began to slow, falling to 85 µm/d by day 80, with full maturity by 24 wk. Compared with rats, rabbits mature more slowly, reaching maturity by 34 wk of age. A study involving 17 male and 12 female NZW rabbits assessed growth of the tibia and femur, assessing the correlation of tibial and femoral lengths and sexual maturity in rabbits.[39] This knowledge helps researchers assess the progressive growth and maturity of rabbits as they change from juvenile to adults.[28] This type of assessment may be important for understanding how intramuscular implants calcify in juvenile (6- to 8-mo-old) rabbits.

The NZW rabbit intramuscular model offers a particular advantage for assessing tissue calcification properties. Epinephrine in rabbits had a higher absorbance and diffusion rate when injected intramuscularly compared with subcutaneously.[16] The intramuscular region in rabbits has a rich vascular supply due to the high density in the latissimus dorsi compared with the subcutaneous of either rats or rabbits. The vascular transport mechanisms of muscle allow it to respond to foreign material (such as BHV tissue) more efficiently than the response to subcutaneous implants.[42] The intramuscular region also offers a more mechanically dynamic environment than the static subcutaneous region, better mimicking some of the stresses on a tissue that a BHV tissue might endure when implanted in humans.

Many analytical methods are used to assess the type of calcification that occurs in arteries or bioprosthetic tissue; currently gaining popularity is near-infrared Fourier transform Raman spectroscopy.[34] This method measures light scattered inelastically from photons.[40] Elastically scattered photons have the same energy (frequency) and therefore wavelength as the incident beam. However, a small fraction of light (approximately 1 in 10^7 photons) is scattered at optical frequencies different from, and usually lower than, the frequency of the incident photons. This process of inelastic scattering of photons is called Raman scattering, which can occur with a change in vibrational, or rotational, or electronic energy of the molecule being studied. The difference in energy between the incident photon and the Raman-scattered photon is equal to the energy of a vibration of the scattering molecule, such as calcium or phosphate. A plot of intensity of scattered light versus energy difference is called a Raman spectrum. When used to assess the type of calcification in BHV, Raman spectroscopy has been shown to be effective in analyzing the presence of calcium phosphate species and, when combined with a calcium assay, the relative calcium:phosphate ratios.[6] The most common type of calcification is the mineral hydroxyapatite [$Ca_{10}(PO_4)_6(OH)_2$]. Roughly 70% of all bone is composed of hydroxyapatite.[18] By using Raman spectroscopy (830 nm), hydroxyapatite was found at wavelengths of 960 to 1200 cm^{-1} in human explanted BHV.[33] Other calcium–phosphate combinations found on explanted human heart valves include carbonate apatites, octacalcium, dicalcium, and amorphous calcium phosphates.[8] Nascent calcification in biologic tissues goes through phase transformations of unstable calcium–phosphate salts to more stable calcium phosphate salts, ultimately maturing into hydroxyapatite.[22] Raman spectroscopy can be applied to a variety of different morphologies, giving it a unique advantage when analyzing biologic samples, which are generally mixtures of fluids, tissues, and mineral deposits.[30] Raman analysis requires minimal preparation of biologic samples and is nondestructive to the sample. In the current study, near-infrared Fourier transform Raman spectroscopy was used to detect the presence of calcification in bioprosthetic valves explanted from humans and in bioprosthetic valve tissue from intramuscular rabbit explants.

The objective of this study was to validate the rabbit intramuscular model for assessing the calcification potential of bioprosthetic tissue. The outcome of this study was to assess the length of study (days) necessary to see significant differences in calcification among 3 test groups and 1 control group, compare the type of calcification seen in the rabbit model with that of human valve explants (Raman spectroscopy), and to correlate the rabbit model to human BHV calcification.

Materials and Methods

Tissue preparation for animal implants. Bovine pericardial tissue was acquired from a local slaughter house and treated in a production facility (Edwards Lifesciences, Irvine, CA). The tissue was processed aseptically in a sterile clean room where excess fat and damaged tissue was removed from the pericardial sacks. All material for test and control tissue groups was fixed in 0.625% glutaraldehyde for 14 d and treated with formaldehyde–ethanol–Tween 80 (FET) solution at 3 g/L. Tissues for test groups then were processed a second time in FET solution at either 1 g/L (test group 1) or 10 g/L (test group 2). Treated tissue then was cut into 8-mm discs by using a biopsy punch. The use of FET in the test groups acts as an anticalcification treatment and a bioburden reduction step. Tissue for the control group did not undergo the second FET treatment.

Animals. This study was approved in advance by the institutional animal care and use committee at Edwards Lifesciences and was performed in an AAALAC-accredited facility. Male NZW rabbits (n = 45; age, 8 wk) were acquired from Western Oregon Rabbitry (Philomath, OR). The rabbits were housed individually or in pairs, depending on the size of the rabbits. The rabbits were allowed to acclimate for 6 d after receipt. Before their use in the study, the rabbits' health was evaluated by a trained animal care technician or the attending veterinarian. The rabbits were fed a high-fiber commercial diet (LabDiet 5325, Newco Distributors, Ranch Cucamonga, CA) once daily and received water through an automatic watering system ad libitum. The rabbit room was maintained at 16.7 to 22.2 °C on a 12:12-h photoperiod, and humidity was kept between 30% and 70% with a minimum of 12 to 15 air changes per hour.

Male and female weanling Sprague–Dawley rats (n = 60; age, 21 to 28 d) were acquired from Charles Rivers Laboratories (Hollister, CA.) The rats were housed in pairs until they reached a weight of 500 g, at which time they are housed separately. The rats were housed on hardwood bedding (Sani-Chips, Newco Distributors), and cages were changed on a weekly basis. PVC tubes were placed in each cage for enrichment activities. Before beginning the study, the rats' health was evaluated by a trained animal care technician or the attending veterinarian. The rats were fed a certified rodent diet (LabDiet 5002, Newco Distributors) once daily and were given water through glass bottles. The rat room was maintained on a 12:12-h photoperiod at 17.8 to 26.1 °C, and humidity was kept between 30% and 70% with a minimum of 10 to 15 air changes per hour.

Implantation and explant retrieval of tissue in rats and rabbits. Each rat and rabbit was assigned a number, randomized by using Excel (Microsoft, Redmond, WA), and weighed. At implantation, rats weighed 20.9 to 31.3 g and rabbits weighed 1.8 to 2.7 kg.

All surgery was performed by using aseptic techniques. Anesthesia was induced in rabbits by using ketamine hydrochloride (35 mg/kg IM; Phoenix Pharmaceuticals, Burlingame, CA) and xylazine hydrochloride (2.5 mg/kg IM; Phoenix Pharmaceuticals) and maintained by using isoflurane (2% or to effect; Phoenix Pharmaceuticals) delivered through a face mask. Each rabbit's back was shaved and sanitized by using 0.05% chlorhexidine. An incision was made through the skin and into the latissimus dorsi muscle, and the tissue sample was inserted between the muscle layers. Each rabbit received six 8-mm samples (2 from each control and test group). The rabbits were evaluated for pain postoperatively and the following day by looking for panting, self-inflicted wounds, lethargy, lack of appetite, and lack of activity; flunixin meglumine (0.1 mL IM; Banamine, Schering-Plough, Kenilworth, NJ) was administered as needed to control pain and discomfort. Only 2 rabbits received analgesia

Rabbits were humanely euthanized at 7 ± 2, 14 ± 2, and 30 ± 4 d after implantation by using sodium pentobarbital (1 mL; 390 mg/mL, Virbac, Fort Worth, TX) intravenously. The tissue samples were harvested from the intramuscular region along the spine, examined visually for infection and calcium, placed in 10% buffered formalin, and sent for X-ray evaluation.

Each rat's back was shaved and sanitized by using 0.05% chlorhexidine. Rats were anesthetized with isoflurane (2% or to effect; Phoenix Pharmaceuticals) delivered by face mask. An incision was made through the skin along the rat's back; blunt dissection was used to expose the subcutaneous region. Tissue samples were inserted into the subcutaneous region, and each rat received three 8-mm samples (1 from each control and test group). Rats were observed for signs of pain or discomfort for 48 h after surgery; buprenorphine hydrochloride subcutaneously (0.01 to 0.05 mg/kg; Buprenorphine, Rickett Benckiser, Hull, England) was provided as needed. At 14 ± 2 and 90 ± 4 d after implantation, rats were euthanized in a CO_2 chamber. Tissue samples were harvested from the subcutaneous region along the back, examined for infection and calcium, placed in 10% buffered formalin, and sent for X-ray evaluation (MX20, Faxtitron, Lincolnshire, IL). Radiography of the calcified tissue assists in determining the dilution required before analyzing each sample (see next section).

Calcium analysis. Elemental calcium was analyzed by using atomic absorption spectroscopy (AA200, Spectra, Varian, TX). Each explanted tissue sample was dried by using a lyophilizer and then digested by using HNO_3. The dry weight of each sample was recorded in milligrams. Each sample then was diluted with phosphate buffer to an appropriate amount based on X-ray scoring so that the absorbance fell along the standard curve of the assay and analyzed by atomic absorption spectroscopy. Calcium values are reported as micrograms of calcium per milligram of dry tissue.

Collection of Raman spectroscopy samples. Several ex-vivo spectra of explanted human aortic valve samples and a subset of three 8-mm bovine pericardial tissue disks from intramuscular rabbit explants (day 30) were analyzed by using Fourier transform–Raman spectroscopy. Segments of tissue were cut into approximately 1mm fragments and placed on a glass microslide with 10% formalin solution and sealed with a glass cover slip. At the time of Raman spectral analysis, samples were analyzed (Nexus 6700/NXR FT–Raman Spectrophotometer, ThermoScientific, San Jose, CA) at room temperature. The excitation laser source consisted of a 1064-nm yttrium vanadate (Nd:YVO_4) solid-state laser, a calcium fluorite (CaF_2) beam splitter (13,500 to 1200 cm^{-1}) and an indium–gallium–arsenide detector at room temperature. The Raman spectra of the tissue were processed by using Nicolet Omnic version 8.0 software (ThermoScientific, Waltham, MA). Spectra were collected directly through the glass coverslips without interference. Every spectrum had a 1-min collection time with 8 cm^{-1} spectral resolution. Fourier transform–Raman microscopy has a spatial resolution of 50 µm and no fluorescence interference.

Representative images were taken of the explanted rabbit sample and human valve were obtained by using a stereomicroscope (Wild M8) with a camera head (DS-5M, Nikon,) and control unit (DS-L1, Nikon).

Statistics. Analysis of variance was performed by using Statgraphics (Statpoint Technologies, Warrenton, VA) to compare the differences in mean calcium values between the rat and rabbit at each time point time at the 95% confidence interval ($P < 0.05$).

Results

Calcium analysis. Radiography revealed visible calcification on all explanted samples, with the exception of rat test groups 1 and 2 at day 14 and rat test group 1 at day 90. For all tissue explanted from both rabbits and rats, the control and test group 1 differed significantly ($P < 0.05$; Table 1), as did the control and test group 2. In addition, 2 rabbit explanted samples had fibrous encapsulation, and 5 rat explanted samples showed necrotic tissue, infection, and encapsulation. Infection of the tissue was present at day 90 but not day 14.

Raman analysis. A sharp band at 960 cm^{-1} was considered an indicator of mineralized hydroxyapatite plaque. This spectral feature was reproducible for all 3 human aortic valve samples and intramuscular rabbit 30-d explanted samples. All calcified regions of the valves and intramuscular rabbit implants were verified by X-ray radiographs. Through comparison with the standard library of Raman spectra (Aldrich, Thermo Fisher Scientific, Waltham, MA), the calcified sites were identified as calcium hydroxyapatite, $Ca_{10}(PO_4)_6(OH)_2$ (Figure 1). Traces of organic matrix, such as collagen, were seen in the range of 2800 to 3100 cm^{-1}. Representative images were taken of the explanted rabbit sample (Figure 2) were obtained.

Table 1. Amount of calcium (μg Ca^{2+}/ mg dry tissue; mean ± 1 SD; n = 10 per group) in rat subcutaneous and rabbit intramuscular explanted bioprosthetic tissue as measured by atomic absorption spectroscopy

	Rabbit			Rat	
	7 d	14 d	30 d	14 d	90 d
Control	6.1 ± 7.1	62.1 ± 55.7	63.3 ± 36.5	16.9 ± 20.6	107.6 ± 104.4
Test group 1	4.7 ± 2.4	26.0 ± 30.1	31.4 ± 29.2	0.3 ± 0.2	0.7 ± 0.2
Test group 2	3.8 ± 2.9	13.8 ± 13.7	44.9 ± 35.3	0.6 ± 0.5	21.2 ± 0.2

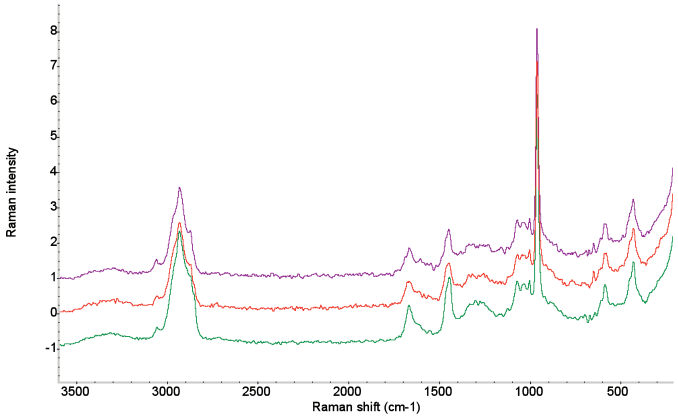

Figure 1. Raman spectral map of intensity versus Raman shift (cm^{-1}) collected from a human explanted valve (purple), rabbit intramuscular explant (red), and the spectrum from the Raman standards library (green).

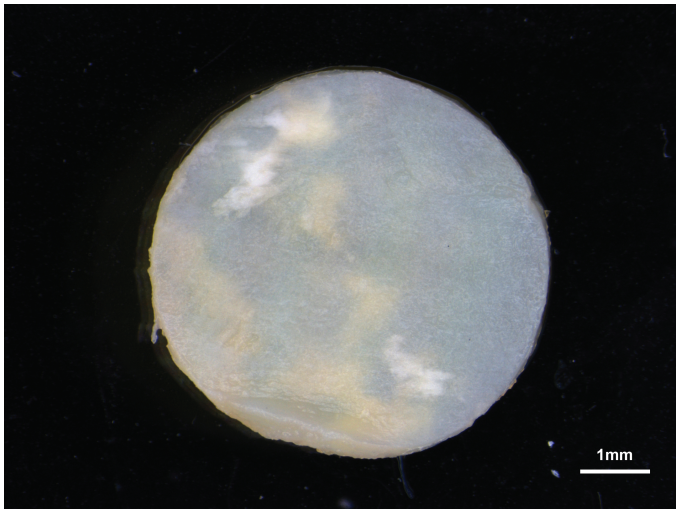

Figure 2. Explanted rabbit intramuscular tissue disc, day 90 (white region indicates hydroxyapatite). Magnification, ×9.

Discussion

Rabbit and rat subcutaneous implants have been used routinely for screening candidate materials for anticalcification for heart valve materials.[31] In 1 report,[31] rabbit subcutaneous implants showed greater calcification at all time points than did the weanling rat model. In addition, intraocular implants tested in subcutaneous and intramuscular sites indicated that the intramuscular implants had greater mineralization.[2] Our current study obtained similar results by using bovine pericardial implants with anticalcification treatments. In all comparable test groups, rabbit intramuscular samples had significantly higher calcium content than did rat subcutaneous samples, and mineralization was apparent at earlier time points in the rabbit model. Given the extremely low levels of calcium seen at day 14, rats were not explanted at day 30. Our results support the conclusion that the rabbit intramuscular model is preferable over the rat subcutaneous model for evaluating calcification at shorter durations. The increased responsiveness of the intramuscular location compared with the subcutaneous may reflect the increased metabolic activity of the muscle, resulting in higher calcium metabolism and deposition.[2] Another advantage of rabbits is that because of their larger body size, more samples can be implanted safely in their intramuscular region and therefore fewer animals are required for each study. In the present study, we implanted 6 samples in rabbits and 3 samples per rat, but 8 to 10 samples can be implanted into a NZW rabbit, and a maximum of 4 samples per animal can be implanted in SD rats.[43]

The results of Raman spectroscopy show a promising way to differentiate normal and calcified tissue in aortic valves and rabbit intramuscular implants. The type of calcification in the rabbit intramuscular samples was identical to that of explanted bioprosthetic valves from human patients. A Raman spectrum can be used to create a molecular fingerprint of a particular tissue and classify its calcification pattern. This process enables 2 different models to be compared with respect to calcification type and structure. For example, in octacalcium phosphate or a similar mineral, the main phosphorus-oxygen stretch occurs at 955 cm^{-1}, whereas in an amorphous calcium phosphate, a broad band occurs at 945 cm^{-1}. In this study, a sharp band at 960 cm^{-1} was an indicator of mineralized hydroxyapatite plaque. In general, the sharpness of the peak can indicate the crystallinity and uniqueness of the mineralization, as opposed to an amorphous or highly-disordered mineralization.[6] The Raman spectra collected in the current study provide a molecular fingerprint of mineralized tissue explants, demonstrating that both the human valve explants and the rabbit intramuscular implants mineralize to form hydroxyapatite.

The rat model had a higher infection rate (5 samples) compared with the rabbit model (0 samples). One of the infected rat explanted samples was cultured and found positive for *Staphylococcus* spp. The cause of infection was unclear, but rats occasionally were seen biting at the implant site. Both the rat subcutaneous and rabbit intramuscular models offer various advantages for assessing the effects of anticalcification treatment on bioprosthetic tissue. In the current study, the unique advantage of the NZW rabbit model was the ability to detect significant differences in calcification much earlier (that is, at 14 d) than in the rat (90 d). Furthermore, because of their size, rabbits can be implanted with more tissue samples than can weanling SD rats. This advantage allows for increasing the number of tissue samples implanted while decreasing the number of animals used. The NZW rabbit model also may offer a more metabolically and mechanically dynamic

environment compared with the static subcutaneous region of the rat model.

The rabbit model correlated well with the human explanted valves, demonstrating that both models calcify over time and produce hydroxyapatite as their final calcium species. Humans continue to regenerate bone until age 65 y; rabbits continue to regenerate bone until 53 mo.[37] This regeneration of bone requires increased levels of bone morphogenic proteins, calcium, phosphate, and multiple hormones, which is why adults younger than 65 y and rabbits younger than 53 mo demonstrate early calcification in bioprosthetic tissue. The rabbit model is just 1 of many choices researchers have regarding assessing the calcification potential of bioprosthetic tissue and efficacy of novel anticalcification treatments.

In conclusion, the study assessed the rabbit intramuscular model as a way of detecting calcification in bioprosthetic tissue. The study showed that the model is robust in detecting and highlighting differences between tissue treated with anticalcification treatments and that treated with glutaraldehyde only.

References

1. **Barnhart GR, Jones M, Ishihara T, Chavez AM, Rose DM, Ferrans VJ.** 1982. Bioprosthetic valvular failure. Clinical and pathological observations in an experimental animal model. J Thorac Cardiovasc Surg **83:**618–631.
2. **Buchen SY, Cunanan CM, Gwon A, Weischenk JI 3rd, Gruber L, Knight PM.** 2001. Assessing intraocular lens calcification in an animal model. J Cataract Refract Surg **27:**1473–1484.
3. **Camilleri JP, Pornin B, Carpentier A.** 1982. Structural changes of glutaraldehyde- treated porcine bioprosthetic valves. Arch Pathol Lab Med **106:**490–496.
4. **Christensen TD, Andersen NT, Attermann J, Hjortdal VE, Maegaard M, Hasenkam JM.** 2003. Mechanical heart valve patients can manage oral anticoagulant therapy themselves. Eur J Cardiothorac Surg **23:**292–298.
5. **Cloft HJ, Kallmes DF, Lin HB, Li ST, Marx WF, Hudson SB, Helm GA, Lopes MB, McGraw JK, Dion JE, Jensen ME.** 2000. Bovine type I collagen as an endovascular stent–graft aterial: biocompatibility study in rabbits. Radiology **214:**557–562.
6. **Delogne C, Lawford PV, Habesch SM, Carolan VA.** 2007. Characterization of the calcification of cardiac valve bioprostheses by environmental scanning electron microscopy and vibrational spectroscopy. J Microsc **228:**62–77.
7. **Eckermann-Ross C.** 2008. Hormonal regulation and calcium metabolism in the rabbit. Vet Clin North Am Exot Anim Pract **11:**139–152 [vii.].
8. **Faure G, Daculsi G, Netter P, Gaucher A, Kerebel B.** 1982. Apatites in heterotopic calcifications. Scan Electron Microsc **4:**1629–1634.
9. **Fishbein MC, Levy RJ, Ferrans VJ, Dearden LC, Nashef A, Goodman AP, Carpentier A.** 1982. Calcifications of cardiac valve bioprostheses. Biochemical, histologic, and ultrastructural observations in a subcutaneous implantation model system. J Thorac Cardiovasc Surg **83:**602–609.
10. **Flameng W, Meuris B, Yperman J, De Visscher G, Herijgers P, Verbeken E.** 2006. Factors influencing calcification of cardiac bioprostheses in adolescent sheep. J Thorac Cardiovasc Surg **132:**89–98.
11. **Giachelli CM.** 2005. Inducers and inhibitors of biomineralization: lessons from pathological calcification. Orthod Craniofac Res **8:**229–231.
12. **Girardot MN, Torrianni M, Girardot JM.** 1994. Effect of AOA on glutaraldehyde-fixed bioprosthetic heart valve cusps and walls: binding and calcification studies. Int J Artif Organs **17:**76–82.
13. **Golomb G, Ezra V.** 1991. Prevention of bioprosthetic heart valve tissue calcification by charge modification: effects of protamine binding by formaldehyde. J Biomed Mater Res **25:**85–98.
14. **Gong G, Ling Z, Seifter E, Factor SM, Frater RW.** 1991. Aldehyde tanning: the villain in bioprosthetic calcification. Eur J Cardiothorac Surg **5:**288–299.
15. **Gross JM.** 2001. Calcification of bioprosthetic heart valves and its assessment. J Thorac Cardiovasc Surg **121:**428–430.
16. **Gu X, Simons ER, Simons KJ.** 1999. Epinephrine absorption after different routes of administration in an animal model. Biopharm Drug Dispos **20:**401–405.
17. **Hammermeister K, Sethi GK, Henderson WG, Grover FL, Oprian C, Rahimtoola SH.** 2000. Outcomes 15 years after valve replacement with a mechanical versus a bioprosthetic valve: final report of the Veterans Affairs randomized trial. J Am Coll Cardiol **36:**1152–1158.
18. **Hedges REM, Van Klinken GJ**. 1992. A review of current approaches in the pretreatment of bone for radiocarbon dating by AMS. Radiocarbon **34:**279–291.
19. **Hunziker EB, Schenk RK.** 1989. Physiological mechanisms adopted by chondrocytes in regulating longitudinal bone growth in rats. J Physiol **414:**55–71.
20. **Koertke H, Hoffmann-Koch A, Boethig D, Minami K, Breymann T, El-Arousy M, Seifert D, Koerfer R.** 2003. Does the noise of mechanical heart valve prostheses affect quality of life as measured by the SF-36(R) questionnaire? Eur J Cardiothorac Surg **24:**52–58.
21. **Langanki D, Ogle MF, Cameron JD, Lirtzman RA, Schroeder RF, Mirsch MW.** 1998. Evaluation of a novel bioprosthetic heart valve incorporating anticalcification and antimicrobial technology in a sheep model. J Heart Valve Dis **7:**633–638.
22. **LeGeros RZ.** 2001. Formation and transformation of calcium phosphates: relevance to vascular calcification. Z Kardiol **90 Suppl 3:**116–124.
23. **Levy RJ, Schoen FJ, Flowers WB, Staelin ST.** 1991. Initiation of mineralization in bioprosthetic heart valves: studies of alkaline phosphatase activity and its inhibition by $AlCl_3$ or $FeCl_3$ preincubations. J Biomed Mater Res **25:**905–935.
24. **Levy RJ, Schoen FJ, Levy JT, Nelson AC, Howard SL, Oshry LJ.** 1983. Biologic determinants of dystrophic calcification and osteocalcin deposition in glutaraldehyde-preserved porcine aortic valve leaflets implanted subcutaneously in rats. Am J Pathol **113:**143–155.
25. **Lomashvili KA, Cobbs S, Hennigar RA, Hardcastle KI, O'Neill WC.** 2004. Phosphate-induced vascular calcification: role of pyrophosphate and osteopontin. J Am Soc Nephrol **15:**1392–1401.
26. **Lund O, Bland M.** 2006. Risk-corrected impact of mechanical versus bioprosthetic valves on longterm mortality after aortic valve replacement. J Thorac Cardiovasc Surg **132:**20–26.
27. **Mako WJ, Shah A, Vesely I.** 1999. Mineralization of glutaraldehyde-fixed porcine aortic valve cusps in the subcutaneous rat model: analysis of variations in implant site and cuspal quadrants. J Biomed Mater Res **45:**209–213.
28. **Masoud I, Shapiro F, Kent R, Moses A.** 1986. A longitudinal study of the growth of the New Zealand White rabbit: cumulative and biweekly incremental growth rates for body length, body weight, femoral length, and tibial length. J Orthop Res **4:**221–231.
29. **Parker R, Randev R, Wain WH, Ross DN.** 1978. Storage of heart valve allografts in glycerol with subsequent antibiotic sterilisation. Thorax **33:**638–645.
30. **Pelletier MJ.** 1999. Analytical applications of Raman spectroscopy, p 281–283. Hoboken (NJ): Blackwell Publishing.
31. **Quintero LJ, Lohre JM, Hernandez N, Meyer SC, McCarthy TJ, Lin DS, Shen SH.** 1998. Evaluation of in vivo models for studying calcification behavior of commercially available bovine pericardium. J Heart Valve Dis **7:**262–267.
32. **Rivas R, Shapiro F.** 2002. Structural stages in the development of the long bones and epiphyses: a study in the New Zealand White rabbit. J Bone Joint Surg Am **84:**85–100.
33. **Rocha R, Villaverde AB, Pasqualucci CA, Silveira L, Brugnera A, Costa MS, Pacheco MT.** 2007. Identification of calcifications in cardiac valves by near infrared Raman spectroscopy. Photomed Laser Surg **25:**287–290.

34. **Romer TJ, Brennan JF 3rd, Puppels GJ, Zwinderman AH, van Duinen SG, van der Laarse A, van der Steen AFW, Bom NA, Bruschke AVG.** 2000. Intravascular ultrasound combined with Raman spectroscopy to localize and quantify cholesterol and calcium salts in atherosclerotic coronary arteries. Arterioscler Thromb Vasc Biol **20:**478–483.
35. **Santos PC, Gerola LR, Casagrande I, Buffolo E, Cheung DT.** 2007. Stentless valves treated by the L-hydro process in the aortic position in sheep. Asian Cardiovasc Thorac Ann **15:**413–417.
36. **Simionescu D, Simionescu A, Deac R.** 1993. Mapping of glutaraldehyde-treated bovine pericardium and tissue selection for bioprosthetic heart valves. J Biomed Mater Res **27:**697–704.
37. **Stoker NG, Epker BN.** 1971. Age changes in endosteal bone remodeling and balance in the rabbit. J Dent Res **50:**1570–1574.
38. **Trantina-Yates A, Weissenstein C, Human P, Zilla P.** 2001. Stentless bioprosthetic heart valve research: sheep versus primate model. Ann Thorac Surg **71:**S422–S427.
39. **University of New South Wales** [Internet]. 2007. [cited 18 August 2008].Available at: http://embryology.med.unsw.edu.au/OtherEmb/Rabbit.htm.
40. **van de Poll SWE, Kastelijn K, Schut TCB, Strijder C, Pasterkamp G, Puppels GJ, van der Laarse A.** 2003. Online detection of cholesterol and calcification by catheter-based Raman spectroscopy in human atherosclerotic plaque ex vivo. Heart **89:**1078–1082.
41. **Vasudev SC, Chandy T, Umasankar MM, Sharma CP.** 2001. Inhibition of bioprosthesis calcification due to synergistic effect of Fe/Mg ions to polyethylene glycol grafted bovine pericardium. J Biomater Appl **16:**93–107.
42. **von Recum AF.** 1986. Handbook of biomaterials evaluation, p 298–300. New York (NY): Macmillan.
43. **Wright G, Olin J, Lafrance H.** 2009. Rabbit IM implants. Irvine (CA): Edwards Lifesciences. Forthcoming.